Generation of Novel Single-Chain Antibodies by Phage-Display Technology to Direct Imaging Agents Highly Selective to Pancreatic β- or α-Cells In Vivo

Sandra Ueberberg,[1] Juris J. Meier,[2] Carmen Waengler,[3,4] Wolfgang Schechinger,[1] Johannes W. Dietrich,[1] Andrea Tannapfel,[5] Inge Schmitz,[5] Ralf Schirrmacher,[4] Manfred Köller,[6] Harald H. Klein,[1] and Stephan Schneider[1]

OBJECTIVE—Noninvasive determination of pancreatic β-cell mass in vivo has been hampered by the lack of suitable β-cell–specific imaging agents. This report outlines an approach for the development of novel ligands homing selectively to islet cells in vivo.

RESEARCH DESIGN AND METHODS—To generate agents specifically binding to pancreatic islets, a phage library was screened for single-chain antibodies (SCAs) on rat islets using two different approaches. *1*) The library was injected into rats in vivo, and islets were isolated after a circulation time of 5 min. *2*) Pancreatic islets were directly isolated, and the library was panned in the islets in vitro. Subsequently, the identified SCAs were extensively characterized in vitro and in vivo.

RESULTS—We report the generation of SCAs that bind highly selective to either β- or α-cells. These SCAs are internalized by target cells, disappear rapidly from the vasculature, and exert no toxicity in vivo. Specific binding to β- or α-cells was detected in cell lines in vitro, in rats in vivo, and in human tissue in situ. Electron microscopy demonstrated binding of SCAs to the endoplasmatic reticulum and the secretory granules. Finally, in a biodistribution study the labeling intensity derived from [^{125}I]-labeled SCAs after intravenous administration in rats strongly predicted the β-cell mass and was inversely related to the glucose excursions during an intraperitoneal glucose tolerance test.

CONCLUSIONS—Our data provide strong evidence that the presented SCAs are highly specific for pancreatic β-cells and enable imaging and quantification in vivo. ***Diabetes*** **58:2324–2334, 2009**

From the [1]Department of Internal Medicine I, Division of Endocrinology and Metabolism, Berufsgenossenschaftliches University Hospital Bergmannsheil, Ruhr-University Bochum, Bochum, Germany; the [2]Department of Internal Medicine I, St. Josef-Hospital, Ruhr-University Bochum, Bochum, Germany; the [3]Department of Nuclear Medicine, Hospital of the Ludwig-Maximilians-University, Munich, Germany; the [4]Department of Neurology & Neurosurgery, Lady Davis Institute for Medical Research, McGill University, Montreal, Canada; the [5]Institute for Pathology, Ruhr-University Bochum, Bochum, Germany; and [6]Chirurgische Forschung, Berufsgenossenschaftliches Universitätsklinikum Bergmannsheil, Ruhr-Universität Bochum, Bochum, Germany.

Corresponding author: Stephan Schneider, stephan.schneider@ruhr-uni-bochum.de.

Received 4 May 2009 and accepted 3 July 2009.

Published ahead of print at http://diabetes.diabetesjournals.org on 10 July 2009. DOI: 10.2337/db09-0658.

The ability to noninvasively measure pancreatic β-cell mass in vivo may provide an early diagnostic tool for the diagnosis of type 1 diabetes and potentially promote the development and evaluation of novel therapeutic strategies. However, despite enormous efforts by various groups, none of the approaches tested have permitted a reliable and noninvasive assessment of β-cell mass in humans.

The small size of islets (50–300 μm in diameter), their low abundance (1–2% of pancreatic mass), and their scattered distribution throughout the pancreas create technical challenges for noninvasive imaging of β-cell mass. Because pancreatic islets possess no intrinsic contrast from the surrounding exocrine tissue, imaging techniques have focused on detecting the pancreatic islet with exogenous agents that are preferentially bound or concentrated in islets, and an extensive library of radiolabeled agents has been applied to islet imaging. However, radiolabeled compounds targeting the sulfonylurea receptor (1–5), the presynaptic vesicular acetylcholine transporter (6), and dopamine uptake in synaptic vesicles (7) have not proven to be effective for islet imaging, most likely because of their failure to achieve the required endocrine-to-exocrine binding ratio (>100:1), as suggested by Sweet et al. (8,9). Another proposed strategy to image islets within the pancreas relates to radiolabeled peptides derived from glucagon-like peptide 1 (GLP-1) or its analogues, taking advantage of the observation that the GLP-1 receptor is expressed at a high density in the islets, but not in exocrine cells (10). This approach has proven useful for imaging insulinomas (11), but has not yet been demonstrated to allow for the determination of islet cell mass in healthy humans or patients with diabetes. Harris and colleagues used [^{11}C]DTBZ, a ligand to vesicular monoamine transporter 2 (VMAT2), to image pancreatic islets in rodents and humans (12–14) by the means of positron emission tomography (PET). Although initial results with DTBZ have been rather encouraging (12,13), recent findings suggest that nonspecific, non–β-cell binding of [^{11}C]DTBZ in the pancreas may limit its utility as a β-cell imaging agent in humans (14).

An obvious reason for these difficulties in generating a valuable imaging agent is the paucity of knowledge about potential targets that are exclusively expressed on the β-cell surface. One way to overcome these limitations is to use phage-display technology, a powerful approach for isolating target-specific peptides and antibodies in animals and humans (15,16). Such single-chain antibodies (SCAs)

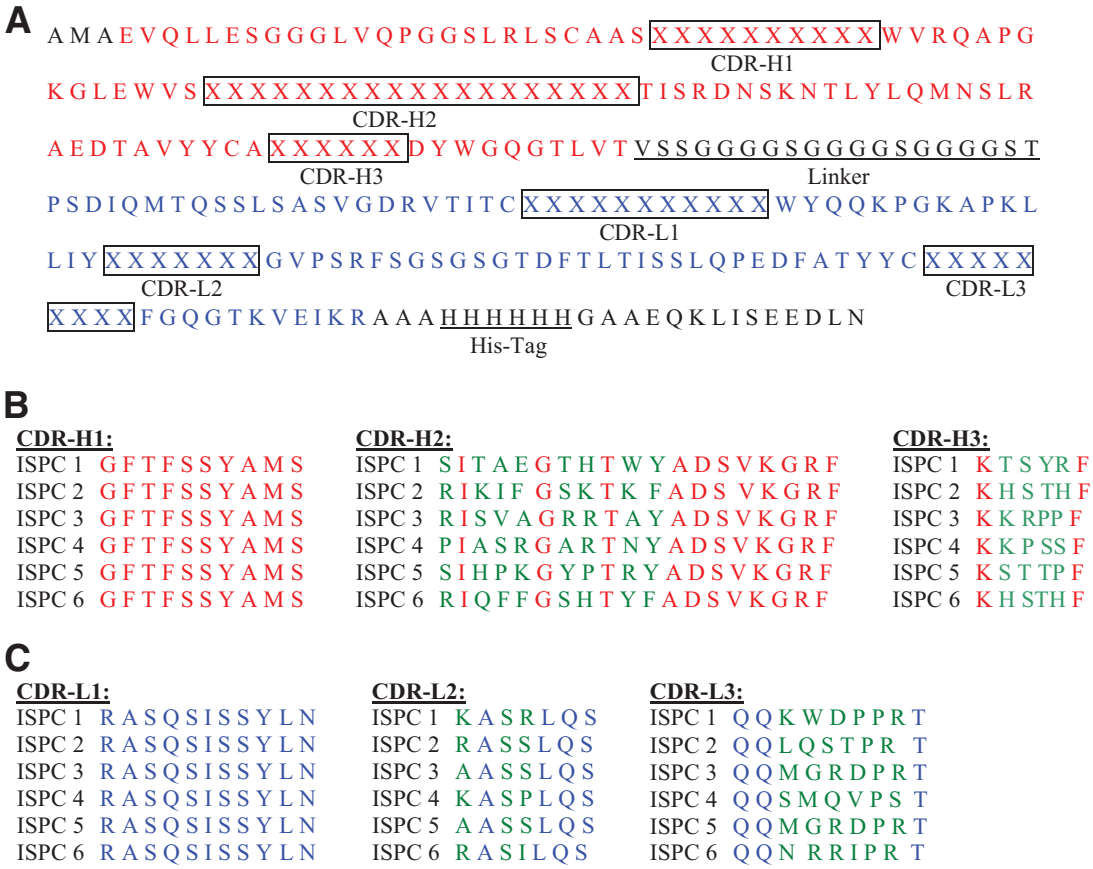

FIG. 1. Shown are the amino acid sequences of the β- and α-cell–specific ISPCs. *A*: Amino acid sequences of heavy (H, red) and light (L, blue) chain. Boxes indicate the CDRs. X = variable amino acids within CDRs. *B* and *C*: Comparison of amino acids within CDR-H1-CDR-H3 (*B*) and within CDR-L1-CDR-L3 (*C*) (variable amino acids are marked in green).

that trigger receptor endocytosis directly have previously been isolated by recovering infectious phages from within cells after receptor-mediated endocytosis (17). For example, internalizing SCAs targeting erbB2 and epidermal growth factor receptor have been identified and used to specifically deliver drugs into breast cancer cells (18,19). Therefore, in the present study, we applied repeated phage panning and rescued the bound phages from within the islet cells to isolate SCAs specifically internalizing in islet β-cells. These SCAs were then further characterized and evaluated with respect to their suitability for islet imaging purposes.

RESEARCH DESIGN AND METHODS

Animal model and human tissue samples. Female CD-rats (6 weeks of age; 200–250 g) received a single intraperitoneal injection of streptozotocin (STZ) 14 days before experiment. To induce different amounts of β-cell mass reduction, rats were treated with either 30 mg/kg (low dose; $n = 5$) or 60 mg/kg (high dose; $n = 5$) STZ. All animal studies were approved by the Landesamt für Naturschutz (Recklinghausen, Germany, no. 50.10.32.08.037). The use of nondiabetic human pancreatic tissue samples was approved by the ethics committee of the Ruhr-University Bochum (no. 2528, amendment 3).

Phage library. The recombinant phage library Tomlinson I is constructed in the pIT2 vector (derived from pHEN1), consists of about 1.4×10^8 different human single-chain variable fragments, and was provided by MRC Geneservice (Cambridge, U.K.). The library is based on a single human framework for VH (V3–23/DP-47 and JH4b) and V (O12/O2/DPK9 and J 1) with diversified (DVT) side chains incorporated in complementarity-determining region (CDR) 2 and CDR 3.

Phage library screening. The library was screened for islet-specific SCAs using two approaches. *1*) For in vivo screening, a nondiabetic CD-rat was injected intravenously through the jugular vein with 10^{12} phage transducing units and allowed to circulate for 5 min. The pancreas was removed, and to recover islet bound phages, the islets were isolated according to a standard protocol except the use of FCS (20). *2*) For in vitro screening, directly isolated rat islets were incubated with 10^{12} phage transducing units for 1 h at 37°C in vitro, as described previously (21). Subsequently, islets from both approaches were treated equally to rescue phages from within the islet cells. Briefly, the islets were washed twice by suspension in 1 ml PBS, followed by lysing the cells by the addition of 1-ml hypotonic solution (30 mmol/l Tris-HCl, pH 8.0) and a single freeze–thaw cycle. Subsequently, the suspension was incubated overnight with TG1 bacteria at 37°C, with transducing units determined to monitor the progress of each round of library panning and the phages amplified according to standard protocols for use in the next round (22).

Purification of SCAs. HB2151 bacteria ($OD_{600} = 0.4$) were infected with 10 μl of isolated phage clones of interest, and colonies were further grown in 2 × TY (100 μg/ml ampicillin and 1% glucose). Isopropyl β-D-thiogalactoside (IPTG; AppliChem, Darmstadt, Germany) was added to induce SCA expression. The supernatant containing the SCAs was purified by metal affinity chromatography (Nunc ProPur, Nunc, Langenselbold, Germany). The purity of the sample was checked by SDS gel electrophoresis and Western blotting.

Immunohistochemistry. Staining of formalin-fixed, paraffin-embedded rat and human tissue sections (5 μm) was performed as follows: Sections were deparaffinized using xylol twice for 10 min and followed by EtOH thrice for 5 min and Aqua dest. for another 5 min. Afterward, the sections were permeabilized by heating in the microwave in antigen unmasking solution pH 6 and down cooling for 45 min. Blocking was done for 1 h at 24°C with PBS containing 2% BSA. Primary and secondary antibodies were diluted in PBS with 2% BSA. Primary antibodies were incubated at 4°C overnight, except for insulin and glucagon with an incubation period of 1 h at 37°C. Secondary antibodies were incubated for 30 min at 24°C, and the same holds true for the Cy2- and Cy3-conjugated streptavidin reagents. The following primary antibodies and dilutions were used: SCA B1 and SCA A1, 1:200; monoclonal mouse anti-c Myc antibody, 1:200 (Cell Signaling, 2276); polyclonal guinea pig anti-swine insulin antibody, 1:400 (Dako, A0564); and monoclonal mouse antiglucagon antibody, 1:200 (Affinity BioReagents, MA1-20210). Secondary antibodies were monoclonal mouse anti-c Myc antibody, 1:200 (Cell Signaling, 2276); biotinylated anti-rabbit IgG and biotinylated anti-mouse IgG, 1:200

(Linaris, BA-1000, BA-2001); Cy3-conjugated goat anti-mouse IgG, 1:200 (Jackson ImmunoResearch Laboratories, 115-165-044); Cy3-conjugated goat anti-guinea pig IgG, 1:800 (Jackson ImmunoResearch Laboratories, 106-165-003). Third reagents were Cy2-conjugated streptavidin, 1:200 (Jackson ImmunoResearch Laboratories, 016-220-084). Tissue slides were analyzed using a Zeiss Axioplan microscope.

Electron microscopy. Rats were transcardially perfused with PBS (2.5% glutaraldehyde) before pancreas extraction, postfixed in 2.5% (wt/vol) glutaraldehyde, rinsed with PBS, postfixed in 1% osmiumtetroxide, dehydrated in ascending concentrations of ethanol and propylenoxide, and embedded in durcupan. Ultrathin sections were incubated with the anti-c Myc antibody (1:100; Cell Signaling, 2276) and a biotinylated anti-mouse IgG, 1:200 (Linaris, BA-2001). Finally, all sections were stained with gold-labeled streptavidin particles (1/20, 10 nm; Aurion, Wageningen, the Netherlands). After rinses, sections were postfixed with 2.0% (wt/vol) glutaraldehyde for 5 min and counterstained. Sections were analyzed on a Zeiss 109 transmission electron microscope.

Labeling SCAs with ^{125}I. The SCAs (0.1 mg) were labeled with ^{125}I using the chloramine-T method as described previously (23).

Cell culture. INS-1 (kind gift from C. Wollheim, Geneva), AR42J (ATCC, Manassas, VA), and α-TC1 cells (ATCC, Manassas, VA) were grown (23,24) and processed as described (23).

Radioactive in vitro assay. The assay was performed as described previously (23), except that an electronic pulse area analysis (CASY Technology, Reutlingen, Germany) was used to estimate the average cell volume (fl). To evaluate specificity of binding, SCAs were preincubated with selected unlabeled SCAs (20 μg) for competition assays.

Pharmacokinetic analysis. Rats injected with 100 μg radiolabeled SCAs were killed at indicated time points, and blood samples were obtained, followed by sedimentation of cellular material and precipitation of supernatant with trichloroacetic acid. Radioactivity associated with pellets and supernatant was measured. Blood content of radiolabel was expressed as a percentage of injected dose per gram of blood (%ID/g).

Intraperitoneal glucose tolerance test. CD-rats received an intraperitoneal glucose tolerance test (IPGTT) 7 days after intravenous injection of SCAs. Rats were fasted for 4 h before the experiments. After baseline blood sampling, animals received an intraperitoneal injection of glucose (2 g/kg body wt) with glucose, insulin, and glucagon levels measured at 30, 60, and 120 min later. Blood samples were taken from tail vein, and glucose was determined by a clinical analyzer (Nova Biomedical, Rödermark, Germany), insulin with ELISA (Mercodia, Uppsala, Sweden), and glucagon with an enzyme immunosorbent assay (Alpco, Salem, NH).

Cell viability and apoptosis. INS-1 or α-TC1 cells (10^6) were exposed overnight to SCAs (5 μg or 20 μg). Apoptosis was assessed with FITC-Annexin-V/propidium iodide (Pharmigen), and analysis was performed with a FACSscan flow cytometer. Viability was determined by staining the cells with calcein-AM (Calbiochem) and propidium iodine (Molecular Probes), photographed with a fluorescence microscope connected to a digital camera, and images were digitally processed using Cell P software (Olympus) and Photoshop 6.0 software (Adobe) (25). Values were compared with those in nontreated controls.

Biodistribution of [^{125}I]-SCA B1, IPGTTs, and estimation of β-cell mass. In this set of experiments, an IPGTT was performed 14 days after diabetes induction (see above for details of these procedures, except that insulin and glucagon levels were not determined) in low-dose STZ (n = 5; fasting plasma glucose [FPG]: 250 ± 10 mg/dl), high-dose STZ (n = 5; FPG: 490 ± 97 mg/dl), and nondiabetic control rats (n = 7; FPG: 90 ± 14 mg/dl). On the following day, the [^{125}I]-SCA B1 (each animal got 0.002 μCi/g of body wt) was injected intravenously in these animals. Two hours after injection, the animals were killed, and pancreases were removed, weighed, and assayed in a gamma counter for radioactivity (26). Accumulation of SCA B1 was expressed as a %ID/g of tissue, corrected for background, and estimated in the glandula parotis. The β-cell mass of the corresponding pancreases was estimated by morphometry (27) according to the following formula: β-cell fraction (%) = insulin-positive area/total pancreatic area; β-cell mass per pancreas (milligram) = β-cell fraction × pancreatic weight (milligram).

Statistics. Curve fits were modeled in form of nonlinear regression. For washout experiments, data were adapted to an exponential decay function with $y = a + b*\exp(-c*x)$, where x denotes the time axis and y the measured count rate. For saturation experiments, results were adapted to an exponential rise function as $y = a + b*(1 - \exp[-c*x])$. Decision criteria were squared regression coefficients (r^2). Parametric comparisons of continuous data were calculated with Student's t test for unpaired data with unequal variance. Main null hypothesis was equal distribution of measured counts in both investigated cell types or with and without preincubation, respectively. Area under the curve (AUC) for glucose, insulin, and glucagon was calculated using the

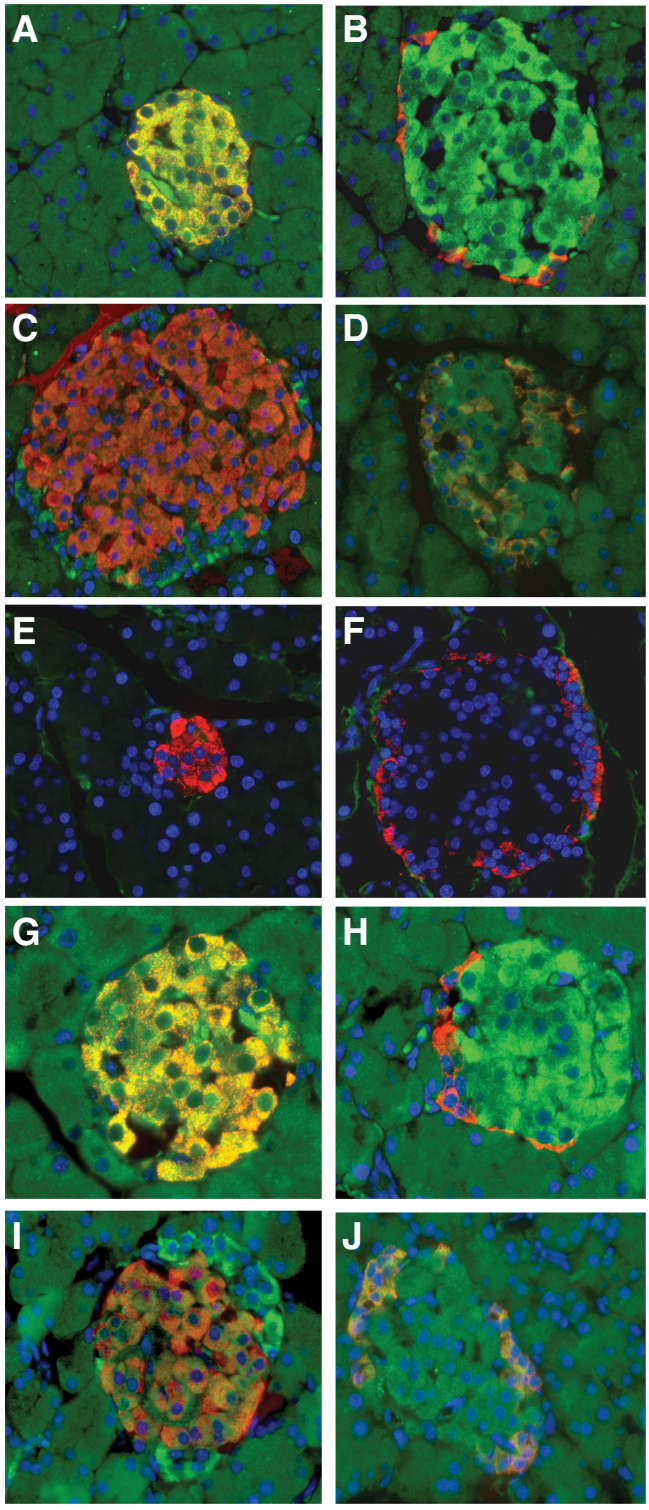

FIG. 2. Immunofluorescence analyses of binding selectivity to pancreatic islets after intravenous application of ISPCs, a control ISPC without an insert, or SCAs in a rat (n = 4 rats per group, 30–40 sections and 60–80 islets per rat). Double staining of ISPCs (*A–F*, green) and insulin (*A*, *C*, and *E*, red) or glucagon (*B*, *D*, and *F*, red) and nucleus using DAPI (blue). The ISPC1 (*A* and *B*) colocalized exclusively with insulin, whereas the ISPC3 (*C* and *D*) colocalized selectively with glucagon. In contrast, the control ISPC without an insert (*E* and *F*) was not detectable in the islets. In another set of experiments, double staining of SCAs (*G–J*, green) and insulin (*G* and *I*, red) or glucagon (*H* and *J*, red) and nucleus using DAPI (blue) was performed. This confirmed the highly selective uptake of SCA B1 in β-cells (*G* and *H*) and of SCA A1 in α-cells (*I* and *J*). All images were acquired at magnification ×40. (A high-quality digital representation of this figure is available in the online issue.)

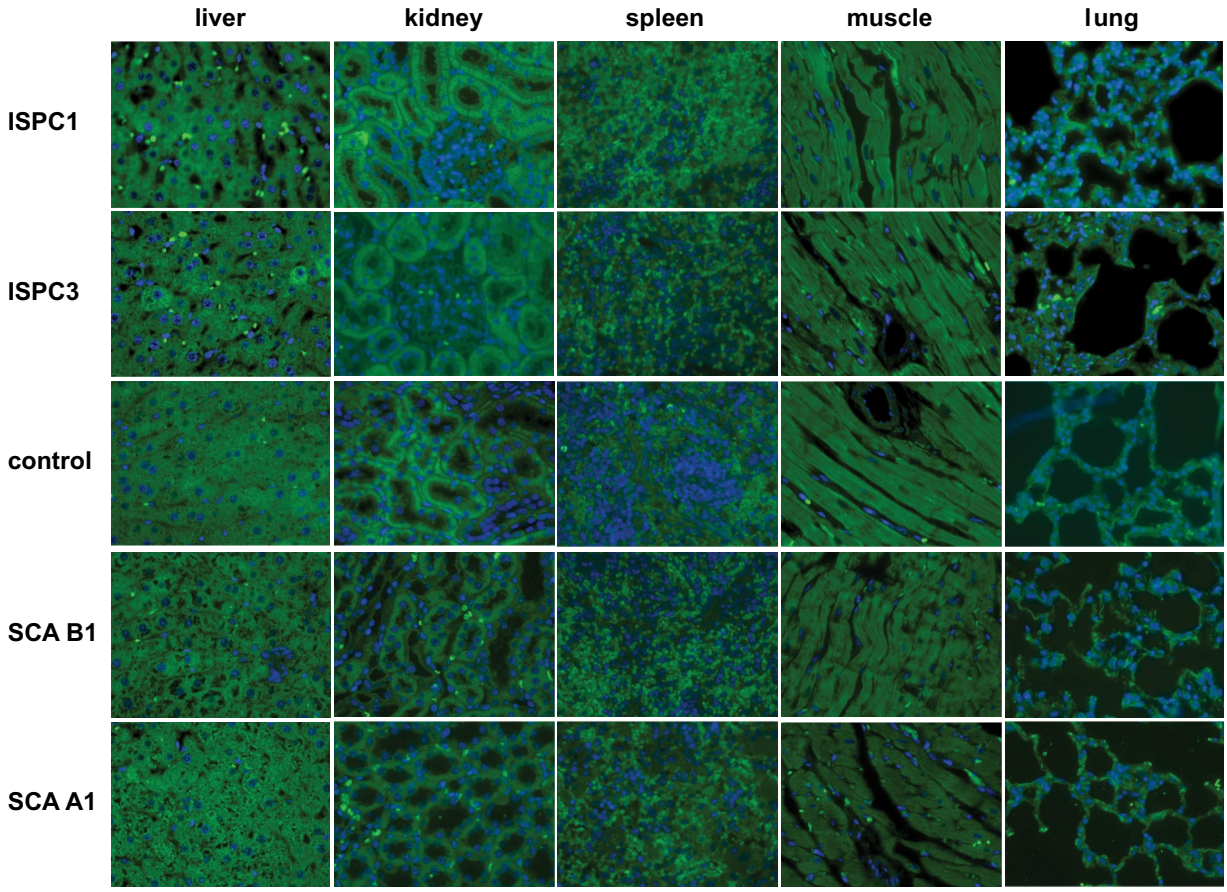

FIG. 3. Immunofluorescence analyses of binding to control tissue after intravenous application of ISPCs, a control ISPC without an insert, or SCAs in a rat (n = 4 rats per group, 30–40 sections per rat). Staining in green color for ISPCs or SCAs. Nuclei were stained with DAPI in blue color. Neither the IPSCs nor SCAs revealed any binding activity to the tested control organs. All images were acquired at magnification ×40. (A high-quality digital representation of this figure is available in the online issue.)

trapezoidal method. All calculations have been performed with KaleidaGraph 4.0.3 for Macintosh Computers (Synergy Software, Reading, PA).

RESULTS

Generation of SCAs binding selectively to either β- or α-cells in rats. To generate agents specifically binding to pancreatic islets, a phage library was screened for SCAs on rat islets using two different approaches: *A*: The library was injected into rats in vivo, and islets were isolated after a circulation time of 5 min. *B*: Pancreatic islets were directly isolated, and the library was panned in the islets in vitro. After five rounds of selection, a marked increase in the phage transducing units per islet over successive rounds of panning was found, demonstrating a 700- and 500-fold enrichment with approach *A* and *B*, respectively. Subsequently, the DNA encoding the corresponding phage-displayed SCAs was sequenced. By these means, four islet-specific phage clones (termed ISPC1 = SCA B1, ISPC2 = SCA B2, ISPC3 = SCA A1, ISPC4 = SCA A2) were identified by approach *A* (Fig. 1). Approach *B* also yielded four ISPCs, two of which were identical to those derived from approach *A* (ISPC1 and 2). The other two ISPCs were termed ISPC5 and 6 (SCA B3 and SCA B4).

Binding selectivity and subcellular localization of SCAs. To determine the binding selectivity of the ISPCs to rat islets in vivo, the ISPCs were injected intravenously and allowed to circulate for 2 h. Subsequently, the animals were killed and the pancreas and control organs were harvested and prepared for immunohistochemical analyses. Immunostaining for ISPC1 was readily detectable in the cytoplasm of islet cells, where it was colocalized to insulin, but not glucagon staining,

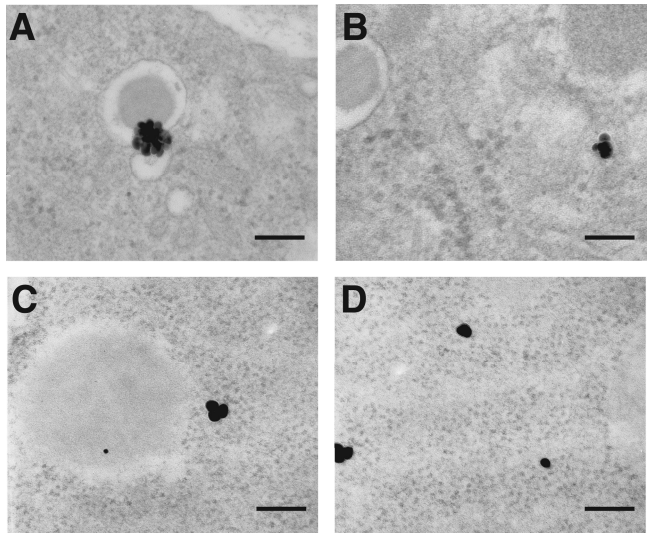

FIG. 4. Ultrastructural analyses of exact intracellular localization of the SCAs after intravenous application in a rat. Transmission electron microscopy detected the β-cell–specific SCA B1 (*A* and *B*) and the α-cell–specific SCA A1 (*C* and *D*) in the endoplasmatic reticulum (*A* and *C*) and at the secretory granule membrane (*B* and *D*) of the respective target cells exclusively (n = 4 rats per group, 20–30 sections per rat). Scale bars, 90 nm.

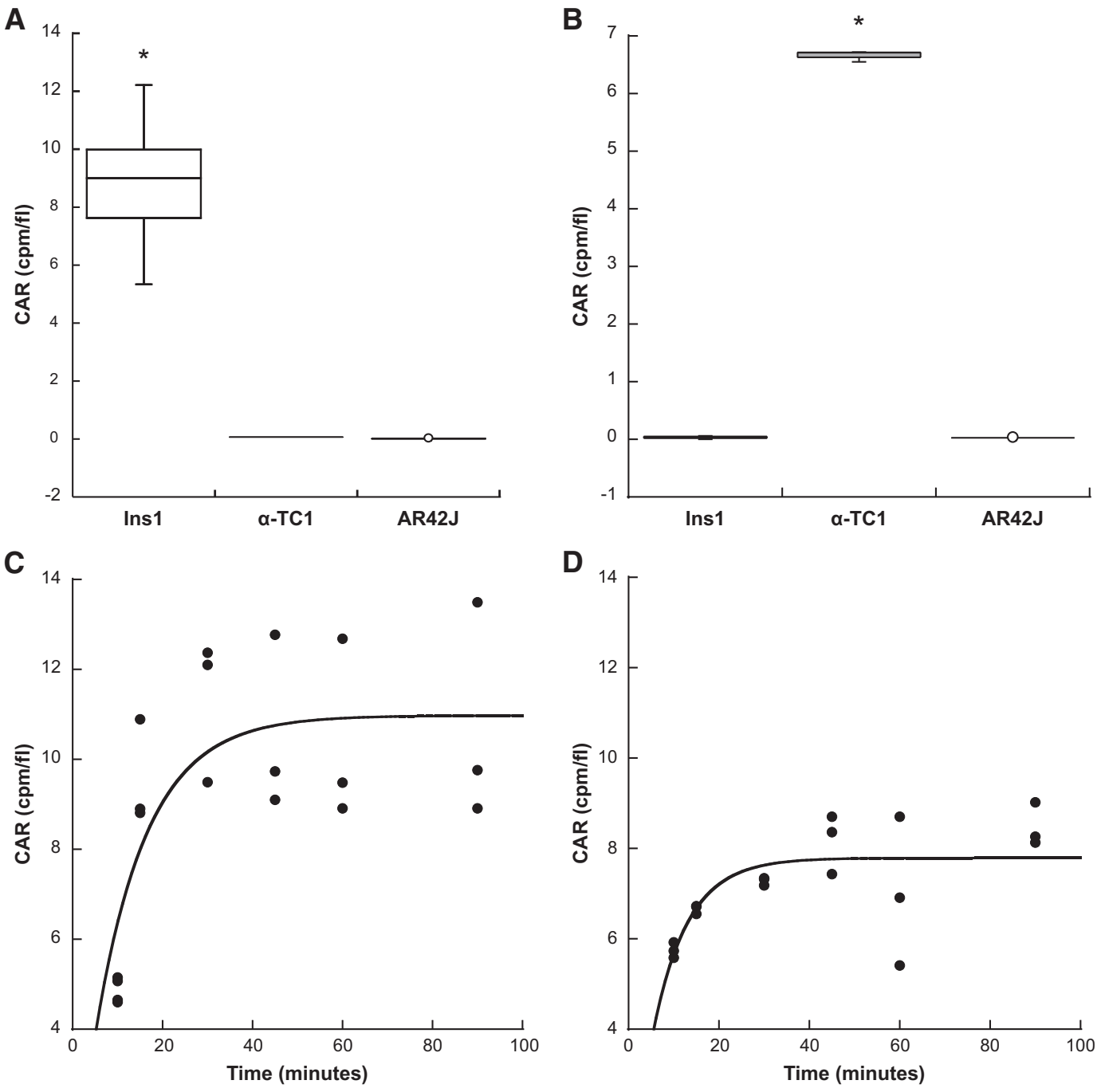

FIG. 5. Analyses of the binding process of selected [^{125}I]-labeled SCAs to different endocrine and exocrine cell lines in vitro and determination of their pharmacokinetic profiles in vivo. Binding specificity of SCA B1 to INS-1 cells (*A*, *P = 0.0016 vs. α-TC1 or AR42J) and SCA A1 to α-TC1 cells (*B*, *P < 0.0001 vs. INS-1 or AR42J). Time course of binding of SCA B1 to INS-1 cells (*C*, $t_{1/2}$ = 8.0 min) or SCA A1 to α-TC1 cells (*D*, $t_{1/2}$ = 5.3 min). Competition assay of SCA B1 (*E*, *P < 0.0001 vs. preincubation (PI) with SCA B1) or SCA A1 (*F*, *P < 0.0001 vs. preincubation with SCA A1) with unlabeled SCAs. Dose response of SCA B1 binding to INS-1 cells (*G*, r^2 = 0.96) or SCA A1 to α-TC1 cells (*H*, r^2 = 0.96). Time course of elimination of SCA B1 (*I*, $t_{1/2}$ = 22.7 min, r^2 = 0.87) or SCA A1 (*J*, $t_{1/2}$ = 19.2 min, r^2 = 0.97) from the vascular system. Error bars represent SEM. CAR, cell-associated radioactivity.

suggesting selective binding to β-cells (Fig. 2*A* and *B*). Similar staining patterns were found for ISPC2, 5, and 6 (data not shown). In contrast, ISPC3 (Fig. 2*C* and *D*) and 4 (data not show) were found to be exclusively colocalized with glucagon staining, indicating that these ISPCs were selectively binding to islet α-cells. Of note, no binding to exocrine cells (Fig. 2*A*–*D*) and several other control organs (liver, kidney, spleen, heart, and lung) was detectable in any of the ISPCs (Fig. 3). Furthermore, control experiments using an ISPC without the insert did not reveal any binding activity to pancreatic islets or other structures (Fig. 2*E* and *F*).

Subsequently, soluble SCAs containing a c-Myc tag and a His_6 tag were generated from all six ISPCs in small-scale cultures. These SCAs were then purified by metal affinity chromatography and administered intravenously into rats. These experiments confirmed the highly selective cytoplasmatic uptake of SCA B1 (Fig. 2*G* and *H*) and B2–4 (data not shown) in β-cells and of SCA A1 (Fig. 2*I* and *J*) and A2 (data not shown) in islet α-cells, whereas no

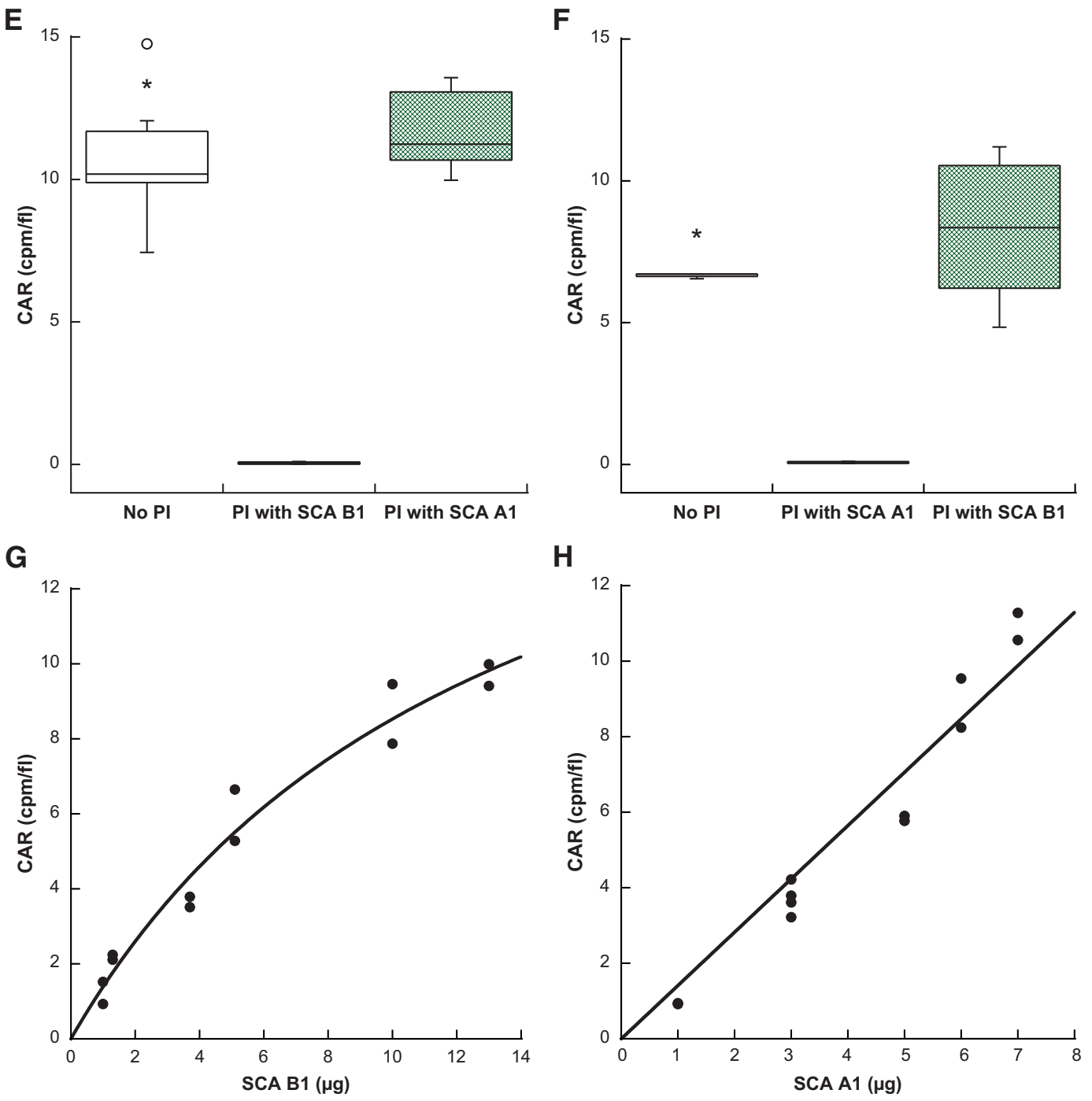

FIG. 5. Continued.

binding to exocrine cells (Fig. 2*G*–*J*) and other control tissues (liver, kidney, spleen, heart, and lung) was detected for any of the SCAs (Fig. 3).

Finally, the SCAs were applied for electron microscopy in rat pancreatic tissue. These analyses confirmed the selective cytoplasmatic localization of SCA B1 and SCA A1 for islet β-cells (Fig. 4*A* and *B*) and α-cells (Fig. 4*C* and *D*), respectively. More specifically, selective binding to the endoplasmatic reticulum and the secretory granules of the respective target cells was found.

Binding properties of radiolabeled SCAs in vitro and pharmacokinetic profiles in vivo. To determine the respective binding properties of selected [^{125}I]-labeled SCAs and to compare these characteristics with other agents examined previously, a systematic in vitro analysis was performed in the β-cell line INS-1, the α-cell line α-TC1, and the exocrine cell line AR42J. Binding of the β-cell–specific SCA B1 to INS-1 cells was 514 times higher than binding to α-TC1 and AR42J cells (Fig. 5*A*). In contrast, the α-cell–specific SCA A1 showed a 210-fold higher binding specificity to α-TC1 relative to INS-1 and AR42J cells (Fig. 5*B*), consistent with the in vivo findings. Furthermore, rapid binding characteristics were found for both SCAs, with a binding half-life of 8.0 min for SCA B1 in INS-1 cells (Fig. 5*C*) and a binding half-life of 5.3 min for SCA A1 in α-TC1 cells (Fig. 5*D*).

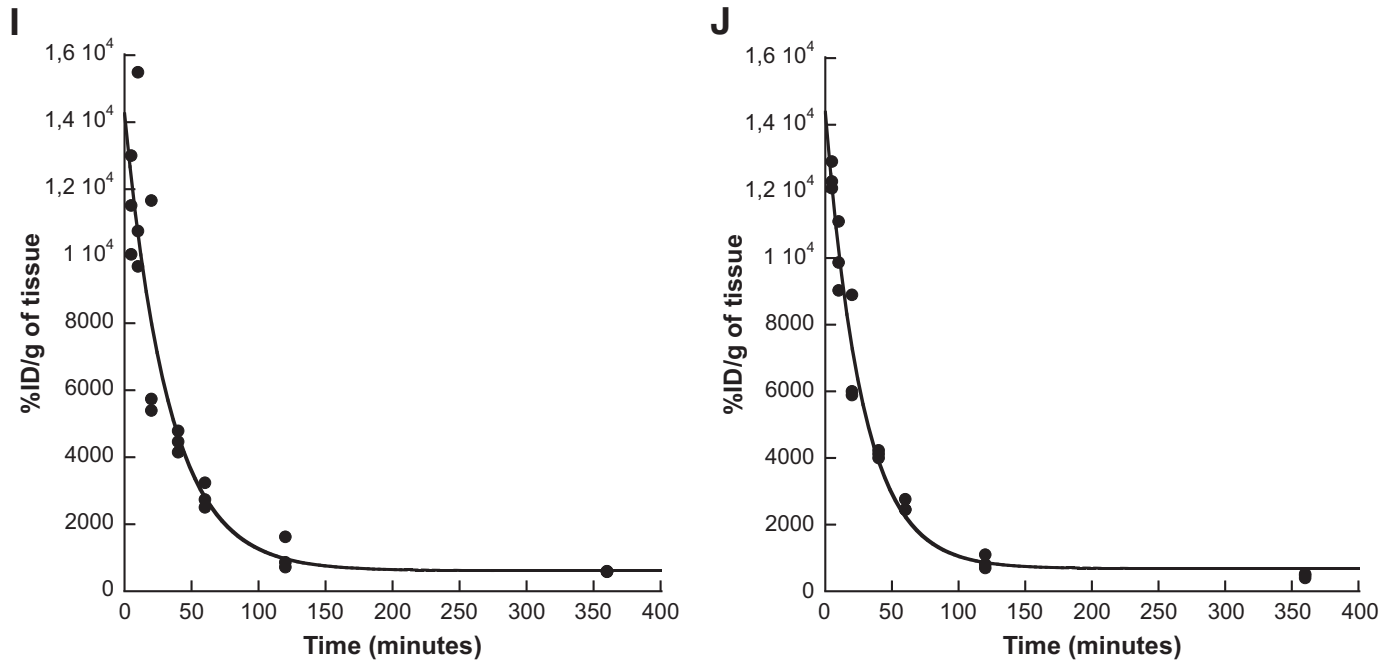

FIG. 5. Continued.

Competition assays demonstrated no binding inhibition of radiolabeled SCA B1 by preincubation with unlabeled SCA A1 and vice versa (Fig. 5*E* and *F*), suggesting that the binding and internalization of these SCAs were mediated by different molecules. For both SCAs, binding saturation could be demonstrated after preincubation with the corresponding unlabeled SCAs (Fig. 5*E* and *F*). The respective dose-response curves revealed a maximum capacity of 650.307 SCA B1 molecules to be internalized per β-cell and of 669.945 SCA A1 molecules to be taken up per α-cell (Fig. 5*G* and *H*).

Because any unbound label circulating in the vasculature might theoretically interfere with the respective imaging signal of the bound label, the plasma clearance kinetics of selected SCAs were determined in rats in vivo (Fig. 5*I* and *J*). For these purposes, preparations of radiolabeled SCAs were administered intravenously into rats, and the respective radioactivity was measured in the plasma over time. These experiments revealed a very rapid elimination of both SCA B1 and SCA A1 from the circulation ($t_{1/2}$ = 22.7 min and 19.2 min, respectively).

Specific binding to human islets in situ. To use these SCAs for the determination of islet cell mass in humans, specific binding to human pancreatic β- or α-cells would be required. Therefore, human pancreatic tissue was costained by immunohistochemistry using the SCAs as well as specific antibodies for insulin and glucagon, respectively. Staining for the β-cell–specific SCA B1 was clearly detectable within the islets and colocalized with insulin expression, whereas no binding to α-cells or exocrine cells was detectable (Fig. 6*A* and *B*). Conversely, the α-cell–specific SCA A1 overlapped with glucagon staining, but neither with insulin staining nor with exocrine cells (Fig. 6*C* and *D*).

In vivo toxicity tests. Because any interference of the SCAs with islet cell function would clearly limit their clinical applicability, IPGTTs were carried out 7 days after the intravenous administration of the SCAs into rats. The time course of plasma glucose, insulin, and glucagon levels during the IPGTT was unchanged by the SCAs compared with vehicle-treated animals (Fig. 7*A–C*), suggesting no impairment in islet function. Furthermore, to rule out direct toxic effects on islet cell turnover, cell viability (Fig. 7*D*) and apoptosis (Fig. 7*E*) were assessed in INS-1 or α-TC1 cells after overnight exposure to increasing amounts of the SCAs in vitro. No influence of islet cell turnover was found in these experiments.

Quantification of β-cell mass using [^{125}I]-SCA B1 in rats. To test the ability of SCA B1 for the quantification of β-cell mass in vivo, 14 days after diabetes induction by STZ treatment, the [^{125}I]-SCA B1 was administered intravenously into rats and allowed to circulate for 2 h. Subsequently, the animals were killed, and the accumulation of

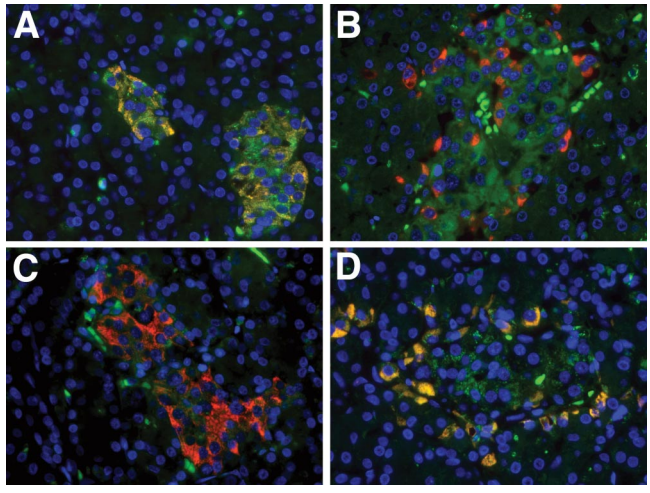

FIG. 6. Immunofluorescent staining for binding of the SCAs to human islets in a pancreas of a nondiabetic subject. SCAs, green; insulin or glucagon, red; DAPI (nucleus), blue. The SCA B1 colocalized selectively with insulin (*A*), but not glucagon staining (*B*). The SCA A1 colocalized with glucagon (*C*), but not insulin-expressing cells (*D*). All images were acquired at magnification ×40. (A high-quality digital representation of this figure is available in the online issue.)

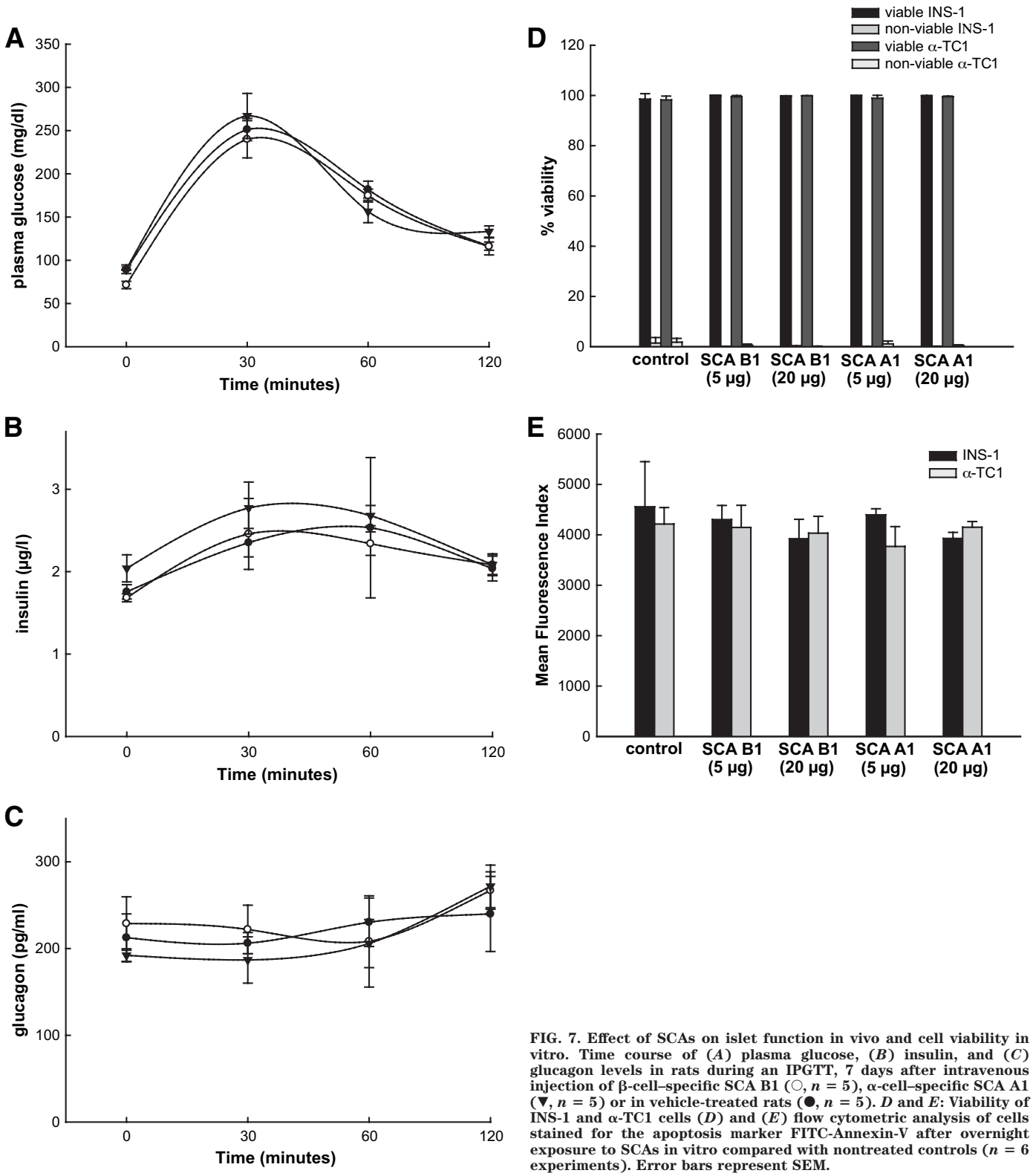

FIG. 7. Effect of SCAs on islet function in vivo and cell viability in vitro. Time course of (*A*) plasma glucose, (*B*) insulin, and (*C*) glucagon levels in rats during an IPGTT, 7 days after intravenous injection of β-cell–specific SCA B1 (○, $n = 5$), α-cell–specific SCA A1 (▼, $n = 5$) or in vehicle-treated rats (●, $n = 5$). *D* and *E*: Viability of INS-1 and α-TC1 cells (*D*) and (*E*) flow cytometric analysis of cells stained for the apoptosis marker FITC-Annexin-V after overnight exposure to SCAs in vitro compared with nontreated controls ($n = 6$ experiments). Error bars represent SEM.

the [^{125}I]-SCA B1 was determined in the harvested pancreas. The measured radiolabeling intensity in the pancreas was then compared with the respective β-cell mass (determined by quantitative morphometry) and the glucose excursions (AUC glucose) during an IPGTT (performed the day before [^{125}I]-SCA B1 application).

Both β-cell mass and the respective radiolabeling intensity were higher in nondiabetic rats than in low- and high-dose STZ-injected diabetic rats (Fig. 8*A*). A strong positive correlation between the radiolabeling intensity of the pancreas and β-cell mass was found within all three subgroups ($r^2 = 0.937$), with the respective probe accumulation diminishing gradually with declining β-cell mass. Furthermore, an inverse relationship between radiolabeling intensity and glucose excursions during the IPGTT was observed ($r^2 = 0.876$, Fig. 8*B*).

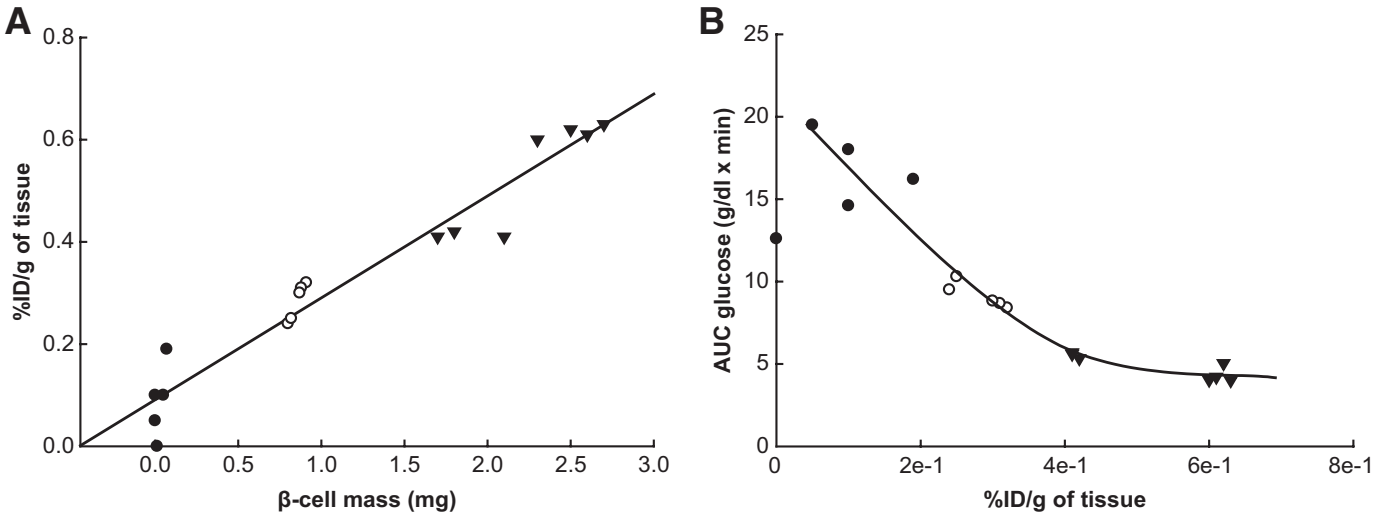

FIG. 8. Correlation of β-cell mass and AUC for glucose during an IPGTT with pancreatic uptake of [^{125}I]-SCA B1 after its intravenous application in a rat. Experiments were performed 14 days after diabetes induction. Linear regression analyses show a close correlation between pancreatic uptake of SCA B1 and β-cell mass in normal (▼), low- (○), and high-dose (●) STZ animals (*A*, $r^2 = 0.937$). Moreover, a strong nonlinear association between the probe accumulation in the pancreas and the AUC for glucose during an IPGTT in the respective animals was depicted (*B*, $r^2 = 0.876$). Each data point represents an animal.

DISCUSSION

We report the successful isolation of six SCAs highly specific for either β- or α-cells both in rodents and in humans. Furthermore, a direct correlation between pancreatic uptake of radiolabeled SCAs and β-cell mass was observed in normal and diabetic animals.

Antibodies have been used for cell-specific delivery of therapeutic compounds, e.g., tumor-specific delivery of chemotherapeutics (28). Therefore, it is reasonable to suppose that antibodies directed against a highly specific β-cell molecule would be of clinical utility for imaging the β-cell mass. In this context, Moore et al. (26) used a [^{111}In]-labeled IC2 antibody, directed against an unknown molecule, which showed excellent correlation between probe accumulation and β-cell mass ex vivo. However, because of the IgM nature of the antibody, a very slow excretion from the vasculature (several days) was evident, leading to an unfavorable signal-to-background ratio in vivo (29). In another study, Ladriere et al. (30) evaluated a [^{125}I]-labeled mouse monoclonal antibody (R2D6) directed against a β-cell surface ganglioside. Although the binding of [^{125}I]-R2D6 was higher in isolated islets than in acinar tissue, no significant difference was detected when comparing islets from normal and rats rendered diabetic by STZ. Recently, Hampe et al. (23) tested another β-cell–specific IgM antibody (K14D10) and concluded that the specificity was far below that required to overcome the signal-to-background ratio in vivo. However, it has been reported that removal of the Fc portion to produce an antibody fragment or an SCA reduces blood clearance time and nonspecific binding (31,32). Therefore, antibody-mediated targeting of β-cells seems to be a promising approach; however, an antibody with excellent binding characteristics, but with a much faster clearance from the vasculature, would need to be developed.

Here, we report the application of a phage-panning approach in rodents to generate SCAs with highly specific binding to pancreatic β-cells in vivo. By these means, we succeeded to isolate four SCAs that are selectively internalized into rodent β-cells in vivo, home to the endoplasmatic reticulum and the insulin secretory granules, and bind to human β-cells in situ. Furthermore, two additional SCAs homing to islet α-cells were identified. These SCAs were highly specific for their respective target cells with no relevant binding to other islet cells, exocrine cells, or other tissues and with a calculated in vitro selectivity of >500:1 for β-cells and >200:1 for islet α-cells. These numbers are far in excess of these reported previously for other potential β-cell mass imaging compounds and meet the requisite exocrine-to-endocrine binding ratio needed to distinguish β-cells (8,9).

Although these studies cannot completely clarify the precise mechanisms subserving the rapid and high-volume (>650,000 SCAs/cell) binding and cellular uptake of SCAs to either β- or α-cells, a membrane receptor-mediated endocytosis appears to be most likely. Moreover, we propose that the intracellular localization of the antibodies has resulted from our screening strategy, which involved lysis and homogenization, meaning that the membrane-bound antibodies were likely eliminated, whereas the intracellular ones were rescued, amplified, and reinjected several times. Such mechanism would be consistent with previous studies in this area in other cell types (17–19,33,34) and would also be consistent with the competitive binding characteristics of different SCAs at β- and α-cells. However, although it seems highly likely that the intracellular uptake of the SCAs was indeed receptor mediated, the specific molecular target remains to be elucidated.

Another important characteristic of the presently described SCAs in favor of a diagnostic application in vivo is the avid elimination of the unbound particles from the circulation. These properties are in line with recent studies showing a rapid elimination of SCAs mainly via the kidneys and have been attributed to their rather low molecular weight (~31 kDa) (32,35).

In addition, this proof of concept study found no alteration of islet turnover or islet function by the respective SCAs. However, more detailed experiments will be required (dose-escalating studies in vivo, repeated applications in vivo, etc.) to completely rule out any toxicity or

antibody formation against the SCAs, before these novel SCAs can be safely applied to humans.

Finally, the SCA B1 tested herein has proven to not only label islet β-cells in vitro or in human pancreas in situ but also provide an excellent tracer for the radiolabeling of β-cells in vivo. Thus, the labeling intensity derived from the [^{125}I]-SCA B1 after intravenous administration in rats in vivo strongly predicted the respective β-cell mass and was inversely related to the glucose excursions during an IPGTT, even though insulin secretion was not directly assessed in this study. Therefore, our data provide strong evidence that the SCAs characterized herein allow for the imaging and quantification of β-cell mass in vivo, which has to be confirmed in future studies using noninvasive imaging techniques such as PET.

In conclusion, we have generated SCAs that bind specifically to β- or α-cells of rodent or human origin and exhibit a high selectivity for their respective target cells over other tissues. These radiolabeled SCAs have proven to reliably predict β-cell mass in rodent models of diabetes after in vivo administration. We propose that such SCAs combined with less invasive imaging techniques, such as PET, may be suitable for the in vivo determination of β-cell mass in humans.

ACKNOWLEDGMENTS

This work was supported by research grants of the Ruhr-University Bochum (FoRUM to S.S. and J.J.M.) and the European Foundation for the Study of Diabetes (EFSD/MSD to S.S. and EFSD/Novartis to H.H.K.).

S.S. and R.S. hold patent application for β-cell imagina. No other potential conflicts of interest relevant to this article were reported.

We thank W. Mier for technical assistance with radioactive labeling of SCAs and S. Herrmann for help with biodistribution studies.

REFERENCES

1. Schirrmacher R, Weber M, Schmitz A, Shiue CY, Alavi AA, Feilen P, Schneider S, Kann P, Rösch F. Radiosyntheses of 1-(4-(2-[^{18}F]fluoroethoxy) benzenesulfonyl)-3-butyl urea: a potential β-cell imaging agent. J Label Compd Radiopharm 2002;45:763–774
2. Schneider S, Feilen PJ, Schreckenberger M, Schwanstecher M, Schwanstecher C, Buchholz HG, Thews O, Oberholzer K, Korobeynikov A, Bauman A, Comagic S, Piel M, Schirrmacher E, Shiue CY, Alavi AA, Bartenstein P, Rösch F, Weber MM, Klein HH, Schirrmacher R. In vitro and in vivo evaluation of novel glibenclamide derivatives as imaging agents for the non-invasive assessment of the pancreatic islet cell mass in animals and humans. Exp Clin Endocrinol Diabetes 2005;113:388–395
3. Schneider S, Ueberberg S, Korobeynikov A, Schechinger W, Schwanstecher C, Schwanstecher M, Klein HH, Schirrmacher E. Synthesis and evaluation of a glibenclamide glucose-conjugate: a potential new lead compound for substituted glibenclamide derivatives as islet imaging agents. Regul Pept 2007;139:122–127
4. Wängler B, Schneider S, Thews O, Schirrmacher E, Comagic S, Feilen P, Schwanstecher G, Schwanstecher M, Shiue CY, Alavi A, Höhnemann S, Piel M, Rösch F, Schirrmacher R. Synthesis and evaluation of (S)-2-(2-[18F]fluoroethoxy)-4-([3-methyl-1-(2-piperidin-1-yl-phenyl)-butyl-carbamoyl]-methyl)-benzoic acid ([18F]repaglinide): a promising radioligand for quantification of pancreatic β-cell mass with positron emission tomography (PET). Nucl Med Biol 2004;31:639–647
5. Wängler B, Beck C, Shiue CY, Schneider S, Schwanstecher C, Schwanstecher M, Feilen PJ, Alavi A, Rösch F, Schirrmacher R. Synthesis and in vitro evaluation of (S)-2-([11C]methoxy)-4-([3-methyl-1-(2-piperidine-1-yl-phenyl)-butyl-carbamoyl]-benzoic acid ([^{11}C]methyl-Repaglinide): a potential β-cell imaging agent. Bioorg Med Chem Lett 2004;14:5205–5209
6. Clark PB, Gage HD, Brown-Proctor C, Buchheimer N, Calles-Escandon J, Mach RH, Morton KA. Neurofunctional imaging of the pancreas utilizing the cholinergic PET radioligand [^{18}F]4-fluorobenzyltrozamicol. Eur J Nucl Med Mol Imaging 2004;31:258–260
7. Otonkoski T, Näntö-Salonen K, Seppänen M, Veijola R, Huopio H, Hussain K, Tapanainen P, Eskola O, Parkkola R, Ekström K, Guiot Y, Rahier J, Laakso M, Rintala R, Nuutila P, Minn H. Noninvasive diagnosis of focal hyperinsulinism of infancy with [18F]-DOPA positron emission tomography. Diabetes 2006;55:13–18
8. Sweet IR, Cook DL, Lernmark A, Greenbaum CJ, Wallen AR, Marcum ES, Stekhova SA, Krohn KA. Systematic screening of potential β-cell imaging agents. Biochem Biophys Res Commun 2004;314:976–983
9. Sweet IR, Cook DL, Lernmark A, Greenbaum CJ, Krohn KA. Non-invasive imaging of β-cell mass: a quantitative analysis. Diabetes Technol Ther 2004;6:652–659
10. Gotthardt M, Lalyko G, van Eerd-Vismale J, Keil B, Schurrat T, Hower M, Laverman P, Behr TM, Boerman OC, Goke B, Behe M. A new technique for in vivo imaging of specific GLP-1 binding sites: first results in small rodents. Regul Pept 2006;137:162–167
11. Wild D, Béhé M, Wicki A, Storch D, Waser B, Gotthardt M, Keil B, Christofori G, Reubi JC, Macke HR. [Lys40(Ahx-DTPA-111In)NH2]exendin-4, a very promising ligand for glucagon-like peptide-1 (GLP-1) receptor targeting. J Nucl Med 2006;47:2025–2033
12. Simpson NR, Souza F, Witkowski P, Maffei A, Raffo A, Herron A, Kilbourn M, Jurewicz A, Herold K, Lui E, Hardy MA, Van Heertum R, Harris PE. Visualizing pancreatic β-cell mass with [11C]DTBZ. Nucl Med Biol 2006; 33:855–864
13. Souza F, Simpson N, Raffo A, Saxena C, Maffei A, Hardy M, Kilbourn M, Goland R, Leibel R, Mann JJ, Van Heertum R, Harris PE. Longitudinal noninvasive PET-based β-cell mass estimates in a spontaneous diabetes rat model. J Clin Invest 2006;116:1506–1513
14. Goland R, Freeby M, Parsey R, Saisho Y, Kumar D, Simpson N, Hirsch J, Prince M, Maffei A, Mann JJ, Butler PC, Van Heertum R, Leibel RL, Ichise M, Harris PE. 11C-dihydrotetrabenazine PET of the pancreas in subjects with long-standing type 1 diabetes and in healthy controls. J Nucl Med 2009;50:382–389
15. Kolonin MG, Saha PK, Chan L, Pasqualini R, Arap W. Reversal of obesity by targeted ablation of adipose tissue. Nat Med 2004;10:625–632
16. Arap W, Kolonin MG, Trepel M, Lahdenranta J, Cardó-Vila M, Giordano RJ, Mintz PJ, Ardelt PU, Yao VJ, Vidal CI, Chen L, Flamm A, Valtanen H, Weavind LM, Hicks ME, Pollock RE, Botz GH, Bucana CD, Koivunen E, Cahill D, Troncoso P, Baggerly KA, Pentz RD, Do KA, Logothetis CJ, Pasqualini R. Steps toward mapping the human vasculature by phage display. Nat Med 2002;8:121–127
17. Roth A, Drummond DC, Conrad F, Hayes ME, Kirpotin DB, Benz CC, Marks JD, Liu B. Anti-CD166 single chain antibody-mediated intracellular delivery of liposomal drugs to prostate cancer cells. Mol Cancer Ther 2007;6:2737–2746
18. Poul MA, Becerril B, Nielsen UB, Morisson P, Marks JD. Selection of tumor-specific internalizing human antibodies from phage libraries. J Mol Biol 2000;301:1149–1161
19. Heitner T, Moor A, Garrison JL, Marks C, Hasan T, Marks JD. Selection of cell binding and internalizing epidermal growth factor receptor antibodies from a phage display library. J Immunol Methods 2001;248:17–30
20. Schneider S, Feilen PJ, Brunnenmeier F, Minnemann T, Zimmermann H, Zimmermann U, Weber MM. Long-term graft function of adult rat and human islets encapsulated in novel alginate-based microcapsules after transplantation in immunocompetent diabetic mice. Diabetes 2005;54:687–693
21. Samli KN, McGuire MJ, Newgard CB, Johnston SA, Brown KC. Peptide-mediated targeting of the islets of Langerhans. Diabetes 2005;54:2103–2108
22. Pasqualini R, Arap W, Rajotte D, Ruoslathi E. In vivo selection of phage display libraries. In *Phage Display: A Laboratory Manual*. Barbas C, Burton D, Silverman G, Scott J, Eds. New York, Cold Spring Harbor Laboratory Press, 2000, p. 22.1–22.24
23. Hampe CS, Wallen AR, Schlosser M, Ziegler M, Sweet IR. Quantitative evaluation of a monoclonal antibody and its fragment as potential markers for pancreatic β-cell mass. Exp Clin Endocrinol Diabetes 2005;113:381–387
24. Powers AC, Efrat S, Mojsov S, Spector D, Habener JF, Hanahan D. Proglucagon processing similar to normal islets in pancreatic α-like cell line derived from transgenic mouse tumor. Diabetes 1990;39:406–414
25. Schildhauer TA, Peter E, Muhr G, Köller M. Activation of human leukocytes on tantalum trabecular metal in comparison to commonly used orthopedic metal implant materials. J Biomed Mater Res A 2009;88:332–341
26. Moore A, Bonner-Weir S, Weissleder R. Non-invasive in vivo measurement of β-cell mass in mouse model of diabetes. Diabetes 2001;50:2231–2236
27. Garofano A, Czernichow P, Bréant B. β-cell mass and proliferation following late fetal and early postnatal malnutrition in the rat. Diabetologia 1998;41:1114–1120

28. Dubowchik GM, Walker MA. Receptor-mediated and enzyme-dependent targeting of cytotoxic anticancer drugs. Pharmacol Ther 1999;83:67–123
29. Schneider S. Efforts to develop methods for in vivo evaluation of the native β-cell mass. Diabetes Obes Metab 2008;10(Suppl. 4):109–118
30. Ladriere L, Malaisse-Lagae F, Alejandro R, Malaisse WJ. Pancreatic fate of a (125)I-labeled mouse monoclonal antibody directed against pancreatic β-cell surface ganglioside(s) in control and diabetic rats. Cell Biochem Funct 2001;19:107–115
31. Colcher D, Pavlinkova G, Beresford G, Booth BJ, Choudhury A, Batra SK. Pharmacokinetics and biodistribution of genetically-engineered antibodies. Q J Nucl Med 1999;43:132–139
32. Holliger P, Hudson PJ. Engineered antibody fragments and the rise of single domains. Nat Biotechnol 2005;23:1126–1136
33. Becerril B, Poul MA, Marks JD. Towards selection of internalizing antibodies from phage libraries. Biochem Biophys Res Commun 1999;255:386–393
34. Lu M, Gong X, Lu Y, Guo J, Wang C, Pan Y. Molecular cloning and functional characterization of a cell-permeable superoxide dismutase targeted to lung adenocarcinoma cells. J Biol Chem 2006;281:13620–13627
35. Müller D, Karle A, Meissburger B, Höfig I, Stork R, Kontermann RE. Improved pharmacokinetics of recombinant bispecific antibody molecules by fusion to human serum albumin. J Biol Chem 2007;282:12650–12660